International Journal of Pharmaceutics 379 (2009) 187–195

Contents lists available at ScienceDirect

International Journal of Pharmaceutics

journal homepage: www.elsevier.com/locate/ijpharm

Pharmaceutical Nanotechnology

Enhancement of gene transfection into human dendritic cells using cationic PLGA nanospheres with a synthesized nuclear localization signal

Takanori Kanazawa, Yuuki Takashima, Motoko Murakoshi, Yuka Nakai, Hiroaki Okada*

Laboratory of Pharmaceutics and Drug Delivery, Department of Pharmaceutical Science, School of Pharmacy, Tokyo University of Pharmacy and Life Sciences, 1432-1 Horinouchi, Hachioji, Tokyo 192-0392, Japan

ARTICLE INFO

Article history:
Received 3 April 2009
Received in revised form 29 May 2009
Accepted 13 June 2009
Available online 23 June 2009

Keywords:
DNA vaccine
Non-dividing dendritic cells
PLGA/PEI nanospheres
Nuclear localization signal
NF-κB p50 analog
Intranuclear transport

ABSTRACT

Effective delivery of DNA encoding antigen into the dendritic cells (DCs), which are non-dividing cells, is very important for the development of DNA vaccines. In a previous study, we developed the PLGA nanospheres that contained a cationic nanomaterial and showed high transfection efficiency in COS7 cells, which divide. In the present study, to produce an effective vector for the DNA vaccines, the gene expression and intracellular trafficking of pDNA complexed with PLGA/PEI nanospheres, in combination with an NF-κB analog as a nuclear localization signal (NLS) and electroporation were evaluated in human monocyte-derived DCs (hMoDCs). Cellular uptake of pDNA both in COS7 cells and hMoDCs was enhanced using the PLGA/PEI nanospheres. On the other hand, the PLGA/PEI nanospheres significantly promoted the transfection in COS7 cells, but had almost no effect on transfection in hMoDCs. The intranuclear transport of pDNA by PLGA/PEI nanospheres in COS7 cells was significantly higher than that in hMoDCs. These results indicate that pDNA complexed with PLGA/PEI nanospheres cannot enter into the nuclei of non-dividing cells. However, PLGA/PEI nanospheres combinated with NLS and electroporation (experimental permeation enhancer) greatly elevated the transfection efficiency by improvement of not only intracellular uptake but also intranuclear transport of pDNA in the hMoDCs. Thus, this delivery system using nanospheres combined with synthesized NLS might be applicable to DC-based gene vaccines when much non-invasive application such as needle-free injector should be required.

1. Introduction

Dendritic cells (DCs), which originate in the bone marrow, are professional antigen-capturing cells and antigen-presenting cells, and these processes initiate the primary immune responses in our body. DCs have unique functions, as they are capable of priming naive T-cells and cross-presenting antigens. One of the characteristics of the DC family is maturation, a process during which they change morphologically and functionally. Immature DCs (iDCs) are phagocytotic cells capable of up-taking antigens at the site of injury or infection. Phagocytosis by DCs is a process that is much more complicated than that by other phagocytotic cells, and allows DCs to present the correct antigenic peptides on MHC class I and II molecules. After processing the antigen, they mature, migrate toward local lymph nodes, and present the antigen to naive T-cells. This central role in cell-mediated immunity has made them an attractive target for cancer immunotherapy (Koido et al., 2000; Rughetti et al., 2000; Landi et al., 2007). DCs loaded with tumor-associated antigens and injected into patients induce anti-tumor responses, which do not occur under natural conditions because of low tumor antigen expression or inaccessibility of antigen to DCs. DCs are also potential vectors for the treatment of chronic infectious diseases, which evade the immune system. Moreover, recent advances in generating DCs have provided strategies for the design of DC-based vaccine (Grunebach et al., 2005). To generate strongly effective DCs, technologies are needed that produce high antigen expression as a result of delivering DNA encoding antigen into the nucleus of DCs, which are non-dividing cells, are needed.

In order to promote the gene expression of pDNA in DCs, the numerous barriers to gene delivery into cells and the nucleus must be overcome. These barriers include (i) cellular adhesion and uptake, (ii) escape from endosomes to the cytoplasm prior to delivery to fusion by lysosomes, (iii) trafficking to the nucleus, and (iv) uptake to the nucleus (Yang et al., 2008). In particular, large foreign molecular substances such as proteins and genes are mostly unable to enter the nucleus of non-dividing cells, in which the nuclear membrane does not disappear upon cell division, since nuclear transfer is strictly controlled by precise machinery.

The nuclear envelope contains nuclear pore complexes (NPCs), which mediate the molecular traffic between the nucleus and cytoplasm. The nucleo-cytoplasmic traffic of large molecules (>25 nm in diameter) is regulated by specific nuclear import and export

* Corresponding author. Tel.: +81 42 676 4490; fax: +81 42 676 4490.
E-mail address: okada@toyaku.ac.jp (H. Okada).

0378-5173/$ – see front matter © 2009 Elsevier B.V. All rights reserved.
doi:10.1016/j.ijpharm.2009.06.015

systems. Proteins that contain classical NLSs are imported into the nucleus by importin α/β heterodimers. Importin α binds to NLS-containing proteins and importin β is responsible for the docking of the importin-cargo complex to the cytoplasmic side of the NPC followed by translocation of the complex through the NPC (Macara, 2001). Classical NLSs consists of a stretch of basic amino acids, arginine and lysine (Morin et al., 1989; Dingwall and Laskey, 1991). Classical NLSs are found in NF-κB p50 and p65 (Gilmore and Temin, 1988; Blank et al., 1991). Recent studies have shown that some signaling molecules are transported into the nucleus by NLS- and importin-independent processes by associating directly with proteins of NPCs (Xu and Massague, 2004). Importin α molecules bind to the previously identified NLSs of NF-κB p50, and NF-κB p50 is bound by the N-terminal NLS binding site of importin α3 (Fagerlund et al., 2005). In addition, we previous reported that a NF-κB p50 analog, a nuclear localizing signal, synthesized in our laboratory, significantly promoted the transfection of pDNA and immune responses on the vaginal membrane (Kanazawa et al., 2008). In a previous study in dividing cells (COS7 cells) (Takashima et al., 2007), we also investigated gene transfection using PLGA nanospheres containing various cationic materials. The obtained PLGA/PEI nanospheres formed strong complexes with pDNA that protected the pDNA from nucleases such as DNase, and the complexes showed significantly higher luciferase expression when compared with other cationic PLGA nanospheres.

In the present study, as a first step toward to a DCs-based gene therapy, the gene expression and intracellular trafficking of pDNA complexed with PLGA/PEI nanospheres in the non-dividing human monocyte-derived DCs (hMoDCs) and dividing COS7 cells were evaluated. Moreover, to optimize the efficiency of delivery into hMoDCs, the transfection efficiency and cellular and intranuclear uptake of pDNA using PLGA/PEI nanospheres combined with the NF-κB p50 analog and electroporation were determined.

2. Materials and methods

2.1. Materials

Plasmid EGFP-N1 (pEGFP, 4.7 kb; BD Biosciences Clontech, USA), which codes for green fluorescence protein, was used as a marker gene. DNA concentration was measured based on UV absorbance at 260 nm. The MURUS Label IT® Cy3 or Cy5 labeling kit (TAKARA BIO Inc., Shiga, Japan) was used for fluorescent labeling of pDNA. PLGA (lactic/glycolic: 75/25, Mw: 14,400, Wako Pure Chemical Industries, Ltd., Osaka, Japan), mannitol (Wako Pure Chemical Industries, Ltd., Osaka, Japan), and polyethyleneimine (PEI, $(C_6H_{21}N_5)_n$, Mw 750 kDa; Sigma–Aldrich Co., USA) were used for preparation of PLGA/PEI nanospheres. Lipofectamine® (Invitrogen, USA) was used as a transfection reagent. The electroporator (Gene Pulser II) was kindly supplied by Bio-Rad Laboratories, Inc. (Tokyo, Japan). Recombinant human GM-CSF and IL-4 for generation of immature DCs were purchased from Wako Pure Chemical Industries, Ltd. (Osaka, Japan). Fluorescein isothiocyanate (FITC)-conjugated anti-CD1a and phycoerythrin (PE)-conjugated anti-CD14 were purchased from eBioscience, Inc. (San Diego, CA, USA). FITC isomer (Wako Pure Chemical Industries, Ltd.), Bio-Gel® P-10 Gel and Polyprep® Chromatography Columns (Bio-Rad Laboratories, Inc. Tokyo, Japan) were used in fluorescently labeling of PEI.

2.2. Preparation of human monocyte-derived immature DCs

Human peripheral blood buffy coat was obtained following informed consent through a protocol approved by Japanese Red Cross Tokyo Metropolitan Blood Center. Peripheral blood monocytes (PBMCs) were isolated by density gradient separation using lymphocyte separation medium (Lymphprep™, AXSIS-SHIELD, USA). PBMCs were then incubated with human CD14-specific antibody conjugated to paramagnetic MicroBeads (Militenyi Biotech, Auburn, CA, USA). $CD14^+$ monocytes were isolated on LS columns (Militenyi Biotech). To generate immature DCs, the $CD14^+$ monocytes were cultured in RPMI containing 10% FBS. After 20 min, non-adherent cells were removed and adherent cells were further cultured with 0.5 ng/mL recombinant human (rh) GM-CSF and 2 ng/mL rhIL-4 for 0–6 days.

The differentiated hMoDCs were characterized by flow cytometory using a FACSCalibur cytometer (Becton Dickinson, San Jose, CA, USA) on days 0, 1, 3, 6. The mAbs used were FITC-conjugated anti-CD1a and PE-conjugated anti-CD14. These mAbs were purchased from eBioscience.

2.3. Cell culture

COS7 cells (African green monkey kidney epithelial-like cells) were maintained at 37 °C and 5% CO_2 in Dulbecco's Modified Eagle Medium (DMEM) containing 10% FBS (GIBCO) and 1% penicillin/streptomycin (stock 10,000 U/mL, 10,000 mg/mL, GIBCO), and were seeded onto 6-well plates at a density of 2×10^5 cells/well (2 mL DMEM). COS7 cells were transfected after 70–80% confluence was reached (~24 h) and were washed with phosphate buffered saline (PBS). hMoDCs were seeded onto 6-well plates at a density of 1×10^6 cells/well (1 mL DMEM), and were transfected after 70–80% confluence was reached (~24 h). Cells were washed with PBS.

2.4. Preparation of PLGA/PEI nanospheres

PLGA/PEI nanospheres (PLGA nanospheres) were prepared by the oil-in-water emulsion solvent-evaporation method in accordance with our previous report (Takashima et al., 2007). Briefly, 120 mL of acetone/methanol mixture (2/1) containing 2 g of PLGA and 1 g of PEI was dropped into 1000 mL of distilled water under constant stirring. After 20 g of mannitol was dissolved in this suspension, the solution was solidified using a spray-dryer (Pulvis Mini-Spry GA32, Yamato Co., Japan). PLGA/PEI nanospheres dispersed in mannitol microspheres were obtained by this process.

2.5. Synthesis of NF-κB and carboxyfluorescein conjugated NF-κB analogs

The NF-κB analog, which consists of Gly and Cys-Gly-NH_2 added to the C and N termini of NF-κB p50 (Table 1), was synthesized as the NLS peptide gene vector using the Fmoc-solid-phase peptide synthesis method with an ABI 433A peptide synthesizer (Applied Biosystems, Japan) as previously reported (Kanazawa et al., 2008). The carboxyfluorescein conjugated NF-κB (CF-NF-κB) analog was synthesized by the condensation reaction. Briefly, the NF-κB analog and carboxyfluorescein were reacted in N-methylpyrolidone, HoBt and carbodiimide reagent overnight. The NF-κB analog and the CF-NF-κB analog were used after purification by reverse-phase HPLC. The molecular weight of the NF-κB analog was determined by matrix-assisted laser desorption ionization time-of-flight mass spectrometry (MALDI-TOFMS): the Mw of NF-κB analog and the CF-NF-κB analog were 1130.36 and 1360.57, respectively.

Table 1
Structure of synthesized NF-κB p50 analog.

Peptide	Sequence
NF-κB analog	Gly-Gln-Arg-Lys-Arg-Gln-Lys-Cys-Gly-NH_2

Underlined sequences were modified from the natural sequence of each peptide.

2.6. In vitro observation of carboxyfluorescein-labeled NF-κB analog

Immature hMoDCs (1×10^6 cells/well) with 1 mL of Opti-MEM I were seeded onto cover glasses in the bottom of 6-well plates and transfected with CF-NF-κB (50 μg) for 4 h. The cells were washed twice with PBS and fixed at room temperature for 10 min with 4% paraformaldehyde, then washed with PBS and mounted with Slow Fade® reagent (Molecular probes Inc., USA) containing the nuclear stain Hoechst33258 (Dojindo Lab., Kumamoto, Japan). Intracellular carboxyfluorescein-NF-κB was observed using fluorescence microscopy (Axiovert 200 M, Carl Zeiss, USA).

2.7. Fluorescent labeling

pEGFP was labeled using the Label IT nucleic acid labeling kit (Mirus Bio LLC, Milwaukee, WI, USA). Following a protocol provided by the manufacturer, 5–50 μL of pEGFP solution (1 mg/mL) and the same amount of Label IT reagent (Cye3 and Cye5) were mixed in 20 mM MOPS buffer (pH 7.5) and incubated at 37 °C for 2 h. Any unreacted labeling reagent was removed and pEGFP was purified by ethanol precipitation.

FITC-conjugated PEI was obtained by adding 150 mg of PEI to 2.5 μmol of FITC isomer solubilized in 5 mL of a 1:1 ethanol/water mixture. The solution was stirred for 30 min at room temperature and FITC-PEI solution was made free of ethanol and finally freeze-dried. In control experiments, the FITC-PEI was dissolved in 1 mM sodium acetate and passed through a BioGel® P10 fine column. The fluorescent material came off the column together with the PEI indicating that the fluorescein was firmly conjugated to the polymer.

2.8. Preparation of pEGFP complexes

pEGFP (1–5 μg) and PLGA/PEI nanospheres complexes were prepared by mixing the two compounds at Mw ratios ranging from 10/1 to 25/1 for 30 min. Lipofectamine (10 μg) and pEGFP (1 μg) complexes were prepared under the same conditions. FITC-PEI and pEGFP (1 μg) complexes were prepared by mixing the two compounds at Mw ratios of 5/1 for 30 min. pEGFP/NF-κB analog (5 μg/50 μg) complexes were prepared by incubation for 30 min. pEGFP/PLGA nanospheres/NF-κB analog triple complexes were prepared by combining pEGFP/NF-κB analog complex and PLGA/PEI nanospheres (50 μg). After a 30-min incubation, the mixture was used for transfection. Complex formation of pEGFP/PLGA nanospheres/NF-κB analog triple complexes was evaluated by gel electrophoresis (1% agarose, TBE buffer, 100 V, 55 min, ethidium bromide staining for 30 min).

2.9. In vitro transfection

COS7 cells (5×10^5 cells) or hMoDCs (1×10^6 cells) were seeded onto 6-well culture plates. After a 24-h incubation in DMEM containing 10% FBS, the cells were rinsed and 1.9 mL of culture medium (Opti-MEM) without FBS was added to each well. pEGFP complex solution (100 μL containing pEGFP: 1–5 μg) was applied to each well with or without electroporation. The electroporation was carried out using a Gene Pulser II unit at 0–900 V with 10 pulses at 25 μF. After 4 h, the medium was removed and replaced with 10% FBS containing DMEM for further incubation. The GFP fluorescence intensity and GFP expression efficiency were measured using flow cytometory. The cells were gated electronically according to the control, non-transfected cells for forward-scatter (FSC) and side-scatter (SSC) properties to induce the main population of the cells and exclude dead cells. The 30,000 events were analyzed using Cell Quest software (BD Biosciences).

2.10. Intracellular amount of Cy5-labeled pEGFP

The Cy5-labeled pEGFP complexes were transfected into the COS7 cells or hMoDCs in a manner similar to the procedure for the *in vitro* transfection. After 4 h incubation, the culture medium was aspirated and the cells were washed twice with PBS. After detachment by pipetting and resuspension in PBS, the cells were analyzed using a flow cytometory. Mock transfection allowed us to define the natural fluorescence limit for COS7 cells or hMoDCs. Thus the Cye5-positive cells and relative fluorescence intensity per cell were determined. The cells were gated electronically according to the control, non-transfected cells for forward-scatter (FSC) and side-scatter (SSC) properties to induce the main population of the cells and exclude dead cells. The 30,000 events were analyzed using Cell Quest software (BD Biosciences).

2.11. Intranuclear amount of Cye5-labeled pEGFP

The Cy5-labeled pEGFP complexes were applied to the COS7 cells or hMoDCs in a manner similar to the procedure for *in vitro* transfection. After 4 h incubation, the culture medium was aspirated and the cells were washed twice with PBS, and then to collect the nuclei, 500 μL of lysis buffer (pH 7.4 10 mM tris(hydroxyl)aminomethane–HCl, 10 mM NaCl, 3 mM $MgCl_2$ and 1% Nonidet P-40) were added to the cells and incubated for 5 min in ice. After collection by centrifugation and resuspension in PBS, the fluorescence intensity of Cye5-pEGFP in the nuclei was analyzed using a microplate reader (Safire Microplate Reader, TECAN). The pEGFP amount in the nuclei was calculated using a calibration curve for Cye5-labeled pEGFP standards. The results show pEGFP amount per nucleus.

2.12. Observation of intracellular trafficking of FITC-PEI and Cye3-pEGFP complex

hMoDCs (1×10^6 cells/well) with 1 mL of Opti-MEM I were seeded onto cover glasses in the bottom of 6-well plates and transfected with the FITC-PEI/Cy3-pEGFP complexes for 4–24 h in a manner similar to the procedure for *in vitro* transfection. The cells were washed twice with PBS and fixed at room temperature for 10 min with 4% paraformaldehyde, washed with PBS and mounted with Slow Fade® reagent (Molecular probes Inc.) containing the nuclear stain Hoechst33258 (Dojindo). Intracellular trafficking of FITC-PEI and Cye3-labeled pEGFP was observed using fluorescence microscopy (Axiovert 200 M, Carl Zeiss, USA) and confocal laser microscopy (FLUOVIEW FV300, Olympus, Tokyo, Japan).

2.13. In vitro cell viability

hMoDCs (2×10^4 cells/well) with 1 mL of Opti-MEM I were seeded into 96 well plates and transfected with the pEGFP complexes for 30 h in a manner similar to the procedure for *in vitro* transfection. The cells were added to MTT reagent, and after 30 h, cell viability was measured using a microplate reader.

2.14. Statistical analysis

All values express the mean ± S.D. Statistical analysis of the data was performed using an unpaired Student's *t*-test. Statistical significance was defined as $^{*}p < 0.05$ and $^{**}p < 0.01$.

3. Results and discussion

3.1. Comparison in COS7 cells and hMoDCs

We previously reported that PLGA nanospheres having of about 120 nm in diameter and +40 mV of zeta potential could form stable pDNA complexes and induce high transfection efficiency in COS7 cells. In general, the transfection efficiency of a non-viral vector obviously decreases in non-dividing cells. In the present study, to assess the potential of applying this method to non-dividing cells, such as hMoDCs, PLGA/PEI nanospheres were transfected into hMoDCs. Fig. 1a shows the GFP expression intensity in COS7 cells and hMoDCs after transfection with PLGA/PEI nanospheres/pEGFP (25 μg/1 μg) and Lipofectamine/pEGFP (10 μg/1 μg) complexes. In COS7 cells, PLGA/PEI nanospheres and Lipofectamine significantly upregulated GFP expression compared with the control. In particularly, the GFP expression intensity of Lipofectamine was the highest. However, a difference in GFP expression intensity between hMoDCs transfected with PLGA/PEI nanospheres and those transfected with Lipofectamine was not observed. To investigate the cause of this result, we determined the intracellular uptake of pEGFP in cells transfected with PLGA/PEI nanospheres and Lipofectamine. The intracellular amounts of pEGFP in COS7 cells and hMoDCs after 4 h transfection with Cye5-labeled pEGFP complex are shown in Fig. 1b. Lipofectamine significantly increased cellular uptake of pEGFP compared to control both in COS7 cells and hMoDCs, and thus the cellular uptake efficiency in COS7 cells and hMoDCs was nearly equivalently. The PLGA/PEI nanospheres also obviously promoted cellular uptake of pEGFP in both of cell types, and in addition, the intracellular amount of pEGFP in hMoDCs was significantly higher than that in COS7 cells. This is most likely due to strong phagocytosis by the DCs which are representative phagocytes as well as macrophages.

We then performed a comparison of induced intracellular uptake of pEGFP was made between cationic PLGA/PEI nanospheres (about 140 nm) and microspheres (about 1 μm). The amount of pEGFP amount in hMoDCs transfected using nanospheres was significantly higher than that using microspheres (data not shown). This result suggests that PLGA/PEI nanospheres are suitable for gene delivery into the DC cytoplasm.

Nuclear transport using PLGA/PEI nanospheres and Lipofectamine in hMoDCs and COS7 cells was next investigated. Fig. 1c shows the intranuclear pEGFP amount in both COS7 cells and hMoDCs 5 h after transfection. In the COS7 cells, the elevation of pEGFP nuclear transport was observed by transfection with both PLGA/PEI nanospheres and Lipofectamine. In contrast, in the hMoDCs, transfection with Lipofectamine and PLGA/PEI nanospheres only slightly increased the intranuclear transport of pEGFP. One possible explanation is that pEGFP complexes cannot easily enter into the nucleus of hMoDCs because the nuclear membrane of hMoDCs is not transitorily broken by cell division, since nuclear transfer is strictly controlled by precise machinery. Taken together, the results shown in Fig. 1 suggest that low transfection efficiency in hMoDCs was due to the low nuclear transport of pEGFP, although PLGA/PEI nanospheres greatly promote cellular uptake of pEGFP in hMoDCs. Theses results clarified that enhancement of nuclear transport efficiency was required to improve the transfection efficiency with PLGA/PEI nanospheres into the hMoDCs.

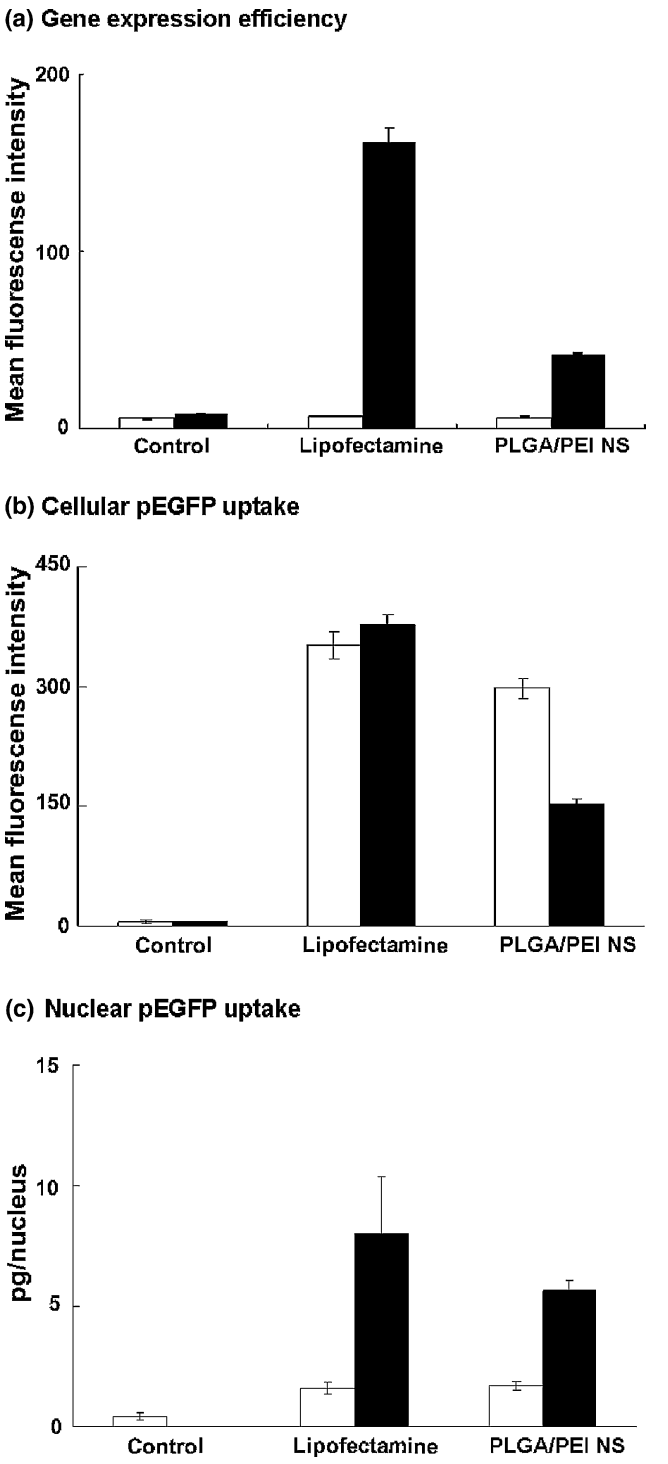

Fig. 1. Transfection efficiency, cellular and nuclear uptake of pEGFP in COS7 cells and MoDCs after transfection with PLGA/PEI nanospheres and Lipofectamine. Lipofectamine (10 μg) or PLGA/PEI nanospheres (PLGA/PEI NS, 25 μg) complexed with 1 μg pEGFP (a) or Cye5 labeled-pEGFP (b and c) was transfected into human monocyte-derived dendritic cells (hMoDCs, open bar) or COS7 cells (closed bar). (a) GFP fluorescence intensity was measured 24 h after transfection. (b) Relative fluorescence intensity per cell was analyzed 4 h after transfection. (c) Intranuclear uptake of Cye5 labeled-pEGFP was measured 5 h after transfection. Control shows data from non-transfected cells. Each bar represents the mean ± S.D. ($n = 3$).

3.2. Intracellular and nuclear trafficking of Cye3-labeled pEGFP in hMoDCs

To clarify the intracellular and nuclear trafficking of pEGFP in hMoDCs, Cye3-labeled pEGFP and FITC-labeled PEI in the cells and nucleus of hMoDCs was also observed by fluorescence microscopy and confocal laser microscopy (Fig. 2). Fig. 2a shows the intracellular trafficking of FITC-PEI (green) and Cye3-pEGFP (red) complex (molar weight ratio of 25:1) 4, 10 and 24 h after transfection into hMoDCs. At 4 h after transfection, yellow, indicating the

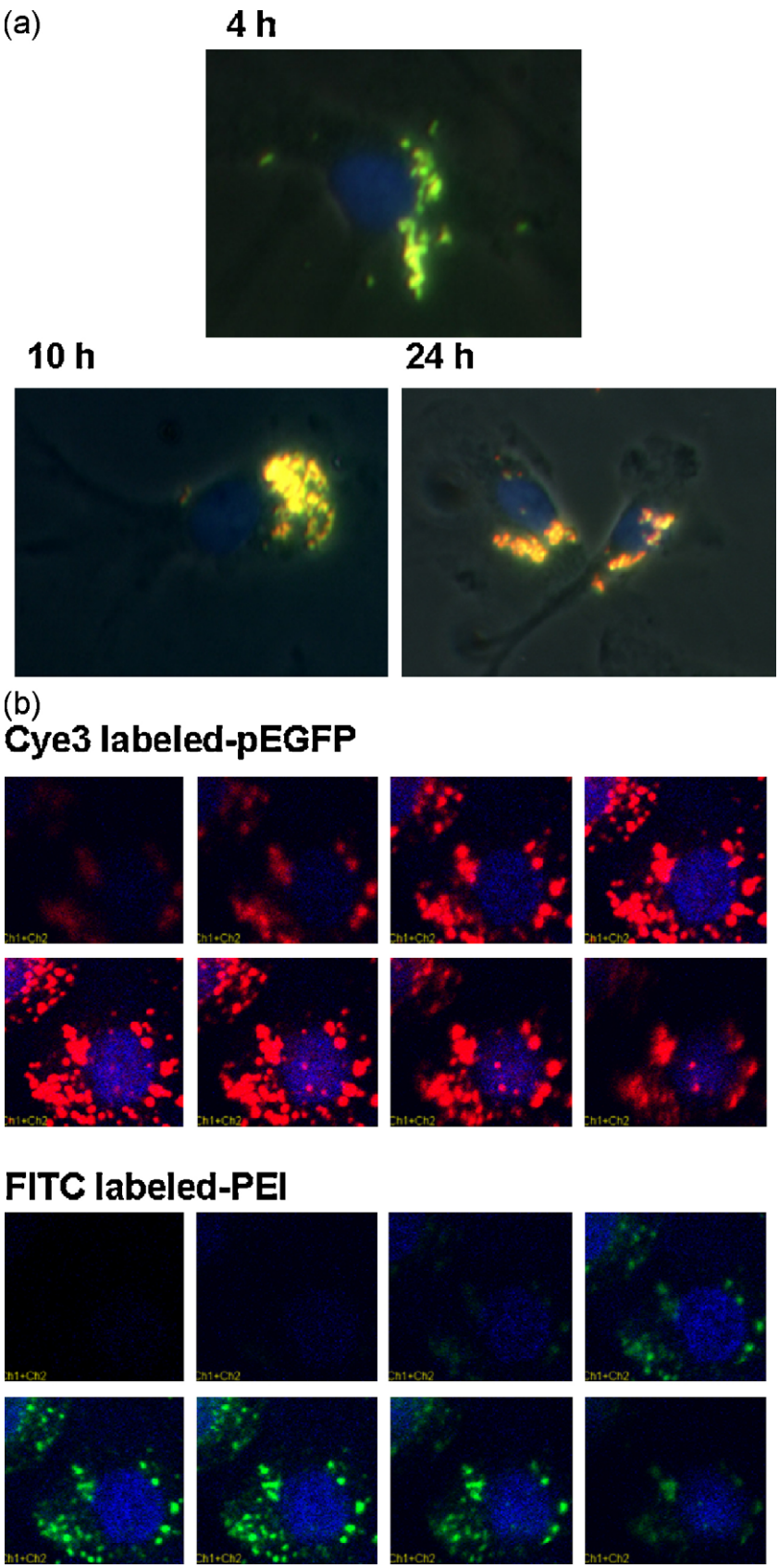

Fig. 2. Intracellular or intranuclear trafficking of Cye3-labeled pEGFP and FITC-labeled PEI in hMoDCs. Cye3-labeled pEGFP (1 μg, red) complexed with FITC-labeled PEI (green) was transfected into hMoDCs. (a) After transfection for 4, 10 and 24 h, the cells were washed twice with PBS and the nuclei were stained with Hoechst 33258 (blue) and observed intracellular trafficking of pEGFP and PEI observed by fluorescence microscopy. (b) After transfection for 4 h, the transfected cells were washed, the nuclei were stained with Hoechst 33258 and intranuclear trafficking of pEGFP and PEI was observed by confocal microscopy. (For interpretation of the references to color in this figure legend, the reader is referred to the web version of the article.)

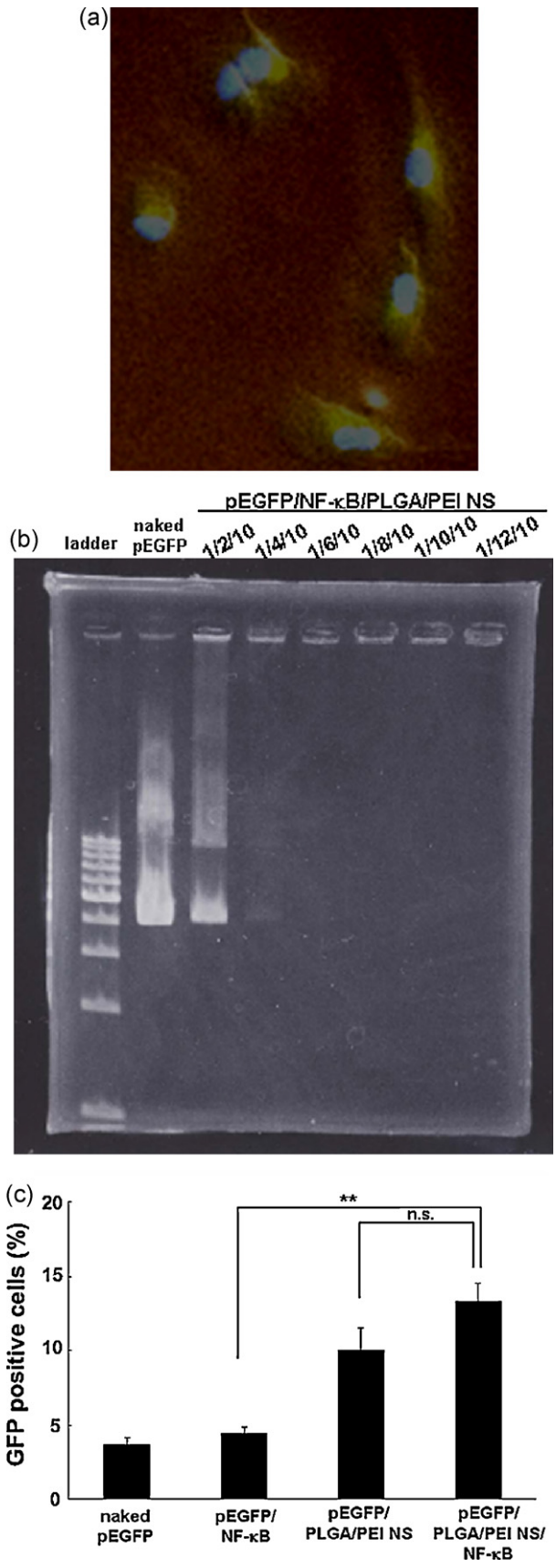

Fig. 3. Effect of a nuclear localization signal, a NF-κB p50 analog, on transfection of pEGFP in hMoDCs. (a) Intracellular trafficking of carboxyfluorescein-labeled NF-κB p50 analog in hMoDCs. Carboxyfluorescein-labeled NF-κB p50 analog (50 μg) was transfected into the hMoDCs and 4 h after transfection, the cells were washed, and the nuclei were stained with Hoechst 33258 (blue) and intracellular trafficking of NF-κB p50 analog (green) observed by fluorescence microscopy. (b) Agarose gel electrophoretic analysis of complex formation of pEGFP with PLGA/PEI NS and NF-κB p50 analog. The 1% agarose gel electrophoresis was carried out in TBE buffer at 100 mV for 40 min and the gel was stained with ethidium bromide. (c) Transfection efficiency of pEGFP in hMoDCs transfected with PLGA/PEI NS and NF-κB p50 analog. PLGA/PEI nanospheres (50 μg) and NF-κB p50 analog (50 μg) complexed with 5 μg pEGFP. GFP expression efficiency was measured 24 h after transfection. Control shows datum of non-transfected cells. Each bar represents the mean ± S.D. ($n = 3$). $^{**}p < 0.01$, $^{n.s.}p > 0.05$. (For interpretation of the references to color in this figure legend, the reader is referred to the web version of the article.)

colocalization of pEGFP (red) and PEI (green), was observed in the cells. This suggests that PEI had localized together with pEGFP in the cells 4 h after transfection. At 10 and 24 h after transfection, some of the yellow had changed to red, suggesting that pEGFP (red) was released from the PEI complex as time after transfection increased. Furthermore, at 24 h after transfection intranuclear localization of some pEGFP was observed.

The intranuclear trafficking of PEI and pEGFP was observed using confocal laser microscopy and is shown in Fig. 2b. The photographs from 1 to 8 represent sliced images from the top to the bottom of the cells. Therefore photographs 6–7 show the center of the cells. A number of the green fluorescently dots indicating PEI were observed in the cells, but were not observed in the blue stained nucleus. In contrast, some red fluorescent dots indicating pEGFP were observed inside the nucleus. These findings indicate that pEGFP was obviously delivered but that PEI was largely unable to enter into the nuclei after being released pEGFP from PEI. The PLGA/PEI nanospheres may show intracellular trafficking similar to PEI because these two vectors are cationic compounds consisting of polymers and cannot easily release pEGFP in the cytoplasm due to the strong ion interaction between the pDNA and vector. These findings suggest that PLGA nanospheres do not have the ability to transport pDNA into the nucleus, and thus the addition of nuclear localization signals was expected to be necessary for high gene expression efficiency in hMoDCs.

3.3. Effect of nuclear localization signals

Our findings indicated that PLGA/PEI nanospheres can strongly deliver pDNA into the cytosol, but not into the nuclei of non-dividing cells such as hMoDCs. In order to improve the nuclear transport efficiency of the PLGA/PEI nanospheres, a nuclear localization signal, a NF-κB p50 analog, was added to the PLGA/PEI nanospheres complexes and transfection then evaluated. First of all, to evaluate the ability of the NF-κB p50 analog itself, the intracellular trafficking of carboxyfluorescein-labeled NF-κB p50 analog at 4 h after transfection was observed by fluorescence microscopy (Fig. 3a). After the transfection, yellow fluorescence indicating the localization of carboxyfluorescein-labeled NF-κB p50 analog inside the Hoechst 33258 labeled-nuclei (blue) was observed as green. This suggested that the NF-κB p50 analog has the ability of nuclear localization. Fig. 3b shows the triple complex formation of PLGA nanospheres and pEGFP/NF-κB p50 analog using agarose gel electrophoresis. The formation of the triple complexes was confirmed by a dose-dependent delay in bands of pEGFP add to PLGA/PEI nanospheres, and then GFP expression in the hMoDCs after transfection with PLGA/PEI nanospheres/pEGFP was increased by the addition of the NF-κB p50 analog. However, as shown in Fig. 3c, the number of GFP-positive cells transfected with PLGA/PEI nanospheres/pEGFP or pEGFP/PLGA nanospheres/NF-κB p50 analog triple complexes at a molecular weight ratio of 1:10 or 1:10:10 was significantly greater than those transfected with naked pEGFP. Although an increase in the elevation of GFP expression efficiency was observed upon the addition of NF-κB p50 analog to the trans-

fection process but was not significant. Furthermore, although the amount of not only cellular but also nuclear uptake of pDNA increased upon addition of NF-κB p50 analog, this elevation was only slight (data not shown). These findings indicated that high transfection efficiency in hMoDCs required further improvement of the cellular and nuclear uptake of pDNA induced by these delivery systems.

3.4. Effect of combination of PLGA/PEI nanospheres, NLS and electroporation

A number of previous reports have shown that electroporation is an effective method for *in vitro* gene transfer by direct delivery into the cytoplasm (Zabner et al., 1995; Lechardeur et al., 1999; Collins et al., 2007). We also expected elevation of pDNA intracellular uptake by electroporation prior to increase of nuclear transport. Therefore, to further improve the DC-gene delivery systems, the combination of PLGA/PEI nanospheres and NF-κB p50 analog with electroporation was investigated.

Fig. 4a shows the GFP expression efficiency in hMoDCs transfected with NF-κB p50 analog/PLGA/PEI nanospheres/pEGFP (10 μg/10 μg/1 μg) with electroporation. In naked pEGFP and pEGFP/NF-κB p50 analog, elevation of GFP expression in hMoDCs by electroporation was not observed. In contrast, in the transfection with pEGFP/PLGA/PEI nanospheres or pEGFP/PLGA/PEI nanospheres/NF-κB p50 analog, combined with electroporation at 300 V, GFP expression obviously increased. In particular, GFP positive cells transfected with pEGFP/PLGA/PEI nanospheres complexed with NF-κB p50 analog were significantly potentiated. This result demonstrated that the elevation of the nuclear transport by NF-κB p50 analog was further increased by increase of cellular uptake by electroporation. However, electroporation at 500 V did not promote gene expression due to the low cell viability that resulted from high-voltage damage. We then evaluated pEGFP cellular uptake into hMoDCs transfected under the same conditions was evaluated (Fig. 4b). The intracellular amount of pEGFP transfected with pEGFP/PLGA nanospheres/NF-κB p50 analog and using electroporation at 300 V increased compared to that without electroporation or without the NF-κB p50 analog, but without PLGA/PEI nanospheres, electroporation seldom induced cellular uptake. It was also clarified the elevation of cellular uptake by using some vector such as PLGA/PEI nanospheres, cell penetrating peptide (Takashima et al., 2007; Kanazawa et al., 2008) and electroporation prior to nuclear localization was essential.

The amino acid sequence of the NLS, containing the NF-κB p50 analog, contains a high percentage of basic amino acids; practically all NLSs identified since have been found to contain a high proportion of cationic amino acids. Therefore, such peptides can serve several roles, such as potential nuclear signaling moieties and the formulation of positively charged pDNA complexes (Conary et al., 1996; Aronsohn and Hughes, 1997; Collins et al., 2007). The modestly up-regulation of pEGFP cellular uptake upon the addition of NF-κB p50 analog in the present study was due to an increase in complex attachment to the cell membrane by positively charged amino acids. These results suggest that the elevation of GFP expression upon the addition of electroporation was due to enhancement of pEGFP cellular uptake not only with PLGA/PEI nanospheres but also with NF-κB p50 analog.

The intranuclear pEGFP amount at for 4 h after transfection under the same conditions in hMoDCs was also determined (Fig. 4c). PLGA/PEI nanospheres/pEGFP and pEGFP/PLGA/PEI nanospheres/NF-κB p50 analog with electroporation at 300 V significantly elevated pEGFP nuclear transport compared to no electroporation, suggesting that electroporation has the ability of potentiation of not only cellular but also nuclear import of pDNA.

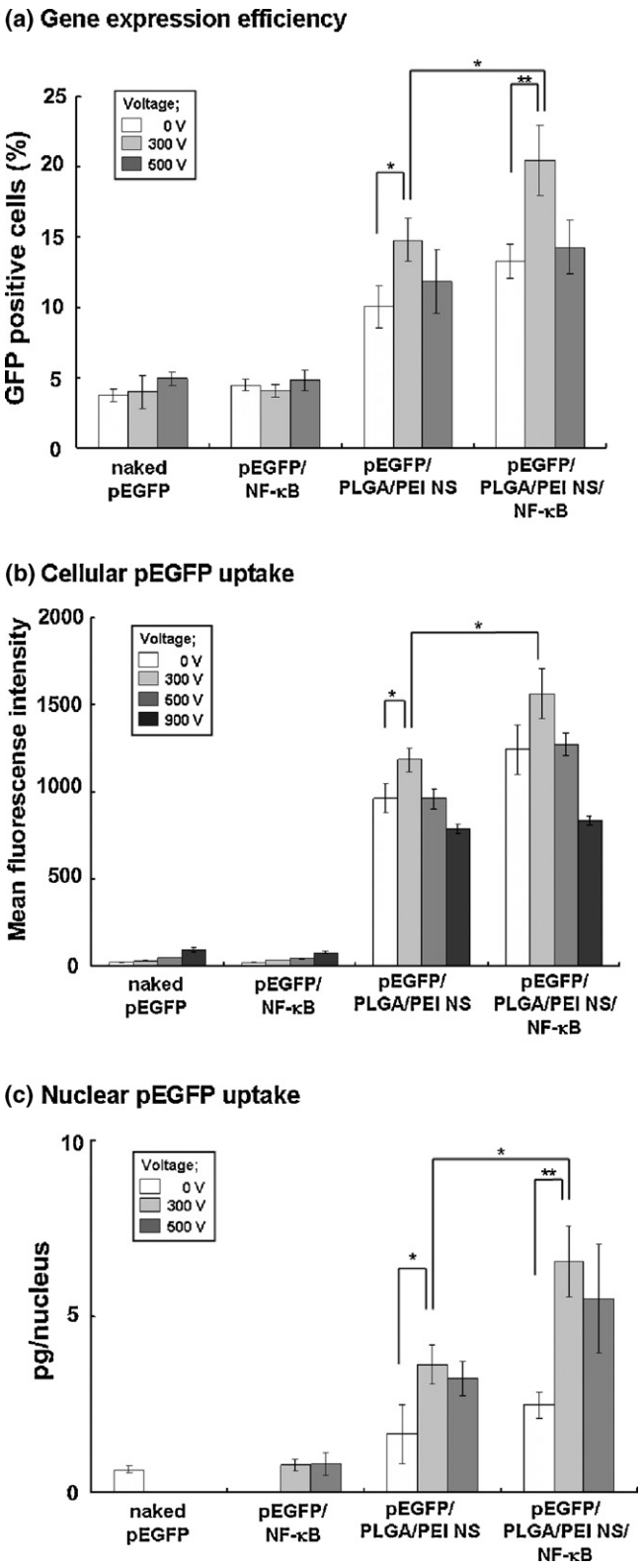

Fig. 4. Transfection efficiency, cellular and nuclear uptake of pEGFP in hMoDCs after transfection with PLGA/PEI nanospheres and Lipofectamine. The naked pEGFP (5 μg), pEGFP/NF-κB p50 analog (5 μg/50 μg), pEGFP/PLGA/PEI NS (5 μg/50 μg) and pEGFP/PLGA/PEI NS/NF-κB p50 analog (5 μg/50 μg/50 μg) were transfected with electroporation at 0–500 V, 10 pulses and 25 μF into the hMoDCs. (a) pEGFP, (b and c) Cye5 labeled-pEGFP. (a) The percentage of GFP-positive cells was measured 24 h after transfection. (b) Relative fluorescence intensity per cell was analyzed 4 h after transfection. (c) Intranuclear uptake of Cye5 labeled-pEGFP was measured 4 h after transfection. Control shows data in non-transfected cells. Each bar represents the mean ± S.D. ($n = 3$). $^{**}p < 0.01$, $^{*}p < 0.05$.

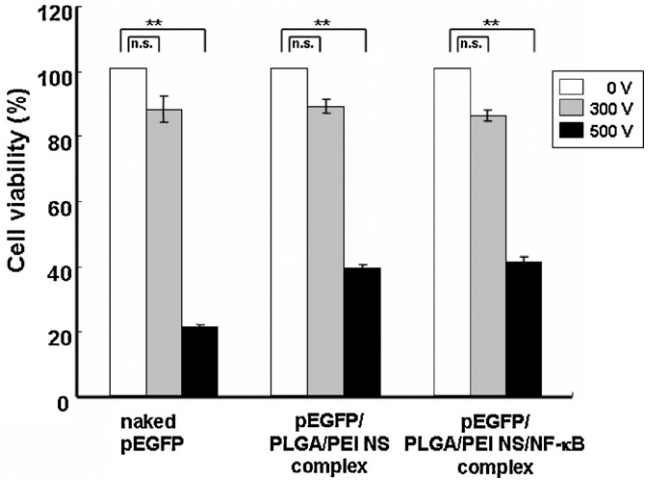

Fig. 5. *In vitro* cytotoxicity of PLGA/PEI NS, NF-κB p50 analog and electroporation in hMoDCs. The naked pEGFP (5 μg), pEGFP/NF-κB p50 analog (5 μg/50 μg), pEGFP/PLGA/PEI NS (5 μg/50 μg) and pEGFP/PLGA/PEI NS/NF-κB p50 analog (5 μg/50 μg/50 μg) were transfected with electroporation at 0–500 V, 10 pulses and 25 μF into the hMoDCs. The MTT assay was performed 30 h after transfection. Each bar represents the mean ± S.D. ($n = 3$). $^{**}p < 0.01$, $^{n.s.}p > 0.05$.

In particular, the intranuclear pEGFP amount in hMoDCs transfected with pEGFP/PLGA nanospheres with the NF-κB p50 analog combined with electroporation was highest among all conditions tested, indicating that the NF-κB p50 analog induces highly efficient intranuclear transport of pDNA following the elevation of intracellular uptake.

Fig. 5 shows the *in vitro* cytotoxicity using the MTT assay of these delivery systems which comprised combination of PLGA/PEI nanospheres, NF-κB p50 analog and electroporation under various conditions. The cell viability at 500 V significantly decreased compared with non-electroporated cells. However, hMoDCs transfected at 300 V, which had the highest GFP expression efficiency, showed low cytotoxicity. These findings indicate that this delivery system is a viable non-viral gene vector even in non-dividing cells such as hMoDCs by development of much safer and well-controlled generation of electroporation. Furthermore, in this study, electroporation was utilized as a cellular permeation enhancer of nanoparticle gene vector, but this method was concerned with cell viability as shown in this study. In our laboratory, we are now developing the newly, much safer and efficient gene delivering system replacing electroporation such as a needle-free injector. In conclusion, it was elucidated the synthesized NLS such as a NF-κB p50 analog could enhance the gene transfection into the non-divided cells such as dendritic cells (APC) by enhancement of gene transfer.

4. Conclusions

Dendritic cells are potential APCs for the treatment of chronic infectious diseases which evade the immune system. Moreover, recent advances in generating DCs have provided strategies for the design of DC-based vaccines. To generate strongly effective DCs, technologies are needed that produce high antigen expression as a result of delivering DNA encoding antigen into the nucleus of DCs, which are non-dividing cells. However, large foreign molecular substances such as proteins and genes are mostly unable to enter the nucleus of non-dividing cells, in which the nuclear membrane does not disappear upon cell division, since nuclear transfer is strictly controlled by precise machinery.

In this study, as a first step toward to DC-based gene therapy, the gene expression and intracellular trafficking of pDNA complexed with PLGA/PEI nanospheres in non-dividing human monocyte-derived DCs (hMoDCs) and dividing COS7 cells were evaluated. Moreover, to develop an efficient delivery system into the non-dividing cells, the transfection efficiency and cellular and intranuclear uptake of pDNA using PLGA/PEI nanospheres combined with a NF-κB p50 analog as a nuclear localization signal (NLS) and electroporation were determined. Intracellular uptake of pDNA using PLGA/PEI nanospheres showed relatively higher efficiency both in COS7 cells and hMoDCs. However, PLGA/PEI nanospheres significantly promoted transfection efficiency in COS7 cells, but did not promote this in hMoDCs, most likely because the intranuclear transport of pDNA by PLGA/PEI nanospheres in COS7 cells was obviously higher than that in hMoDCs. Thus pDNA cannot enter the nucleus of non-dividing cells via this vector. PLGA/PEI nanospheres combined with a NLS greatly elevated the transfection efficiency by improvement of intranuclear transport of pDNA in the non-dividing cells following increase of intracellular uptake. Thus, this synthesized NLS combined with PLGA/PEI nanospheres should be useful in the development of non-toxic, DC-based gene vaccines. However, the development of non-invasive much safer and cellular injector such as a well-controlled electroporator or needle-free injector must be essential to being out the effect of these nuclear transporters.

Acknowledgements

These studies were supported in part by a grant from the Promotion and Mutual Aid Corporation for Private Schools of Japan. The authors would like to thank Advanced (Tokyo, Japan) for the kind supply of the electroporator. We also appreciate Dr. Tsunehiko Fukuda at Nagahama Institute of Bio-Science and Technology for his help in the synthesis of peptides.

References

Aronsohn, A.I., Hughes, J.A., 1997. Nuclear localization signal peptides enhance cationic liposome-mediated gene therapy. J. Drug Target. 5, 163–169.
Blank, V., Kourilsky, P., Israel, A., 1991. Cytoplasmic retention, DNA-binding and processing of NF-κB p50 precursor are controlled by a small region in its C-terminus. EMBO J. 10, 4159–4167.
Collins, E., Birchall, J.C., Williams, J.L., Gumbleton, M., 2007. Nuclear localization and pDNA condensation in non-viral gene delivery. J. Gene Med. 9, 265–274.
Conary, J.T., Erdos, G., McGuire, M., 1996. Cationic liposome plasmid DNA complexes: in vitro cell entry and transgene expression augmented by synthetic signal peptides. Eur. J. Phar. Biopharm. 42, 277–285.
Dingwall, C., Laskey, R.A., 1991. Nuclear targeting sequences—a consensus. Trends Biochem. Sci. 16, 478–481.
Fagerlund, R., Kinnunen, L., Köhler, M., Julkunen, I., Melen, K., 2005. NF-κB is transported into the nucleus by importin α3 and importin α4. J. Biol. Chem. 280, 15942–15951.
Gilmore, T.D., Temin, H.M., 1988. V-rel oncoproteins in the nucleus and in the cytoplasm transform chicken spleen cells. J. Virol. 62, 703–714.
Grunebach, F., Muller, M.R., Brossart, P., 2005. New developments in dendritic cell-based vaccinations: RNA translated into clinics. Cancer Immunol. Immunother. 54, 517–525.
Kanazawa, T., Takashima, Y., Hirayama, S., Okada, H., 2008. Effects of menstrual cycle on gene transfection through mouse vagina for DNA vaccine. Int. J. Pharm. 360, 164–170.
Koido, S., Kashiwaba, M., Chen, D., Gendler, S., Kufe, D., Gong, J., 2000. Induction of antitumor immunity by vaccination of dendritic cells transfected with MUC1 RNA. J. Immunol. 165, 5713–5719.
Landi, A., Babiuk, L.A., van Drunen Little-van den Hurk, S., 2007. High transfection efficiency, gene expression, and viability of monocyte-derived human dendritic cells after nonviral gene transfer. J. Leukocyte Biol. 82, 849–860.
Lechardeur, D., Sohn, K.J., Haardt, M., 1999. Metabolic instability of plasmid DNA in the cytosol: a potential barrier to gene transfer. Gene Ther. 6, 482–497.
Macara, I.G., 2001. Transport into and out of nucleus. Microbiol. Mol. Biol. Rev. 65, 570–594.
Morin, N., Delsert, C., Klessig, D.F., 1989. Nuclear localization of the adenovirus DNA-binding protein: requirement for two signals and complementation during viral infection. Mol. Cell. Biol. 9, 4372–4380.
Rughetti, A., Biffoni, M., Sabbatucci, M., Rahimi, H., Pellicciotta, I., Fattorossi, A., Pierelli, L., Scambia, G., Lavitrano, M., Frati, L., Nuti, M., 2000. Transfected human dendritic cells to induce antitumor immunity. Gene. Ther. 7, 1458–1466.

Takashima, Y., Saito, R., Nakajima, A., Oda, M., Kimura, A., Kanazawa, T., Okada, H., 2007. Spry-drying preparation of microparticles containing cationic PLGA nanospheres as gene carriers for avoiding aggregation of nanospheres. Int. J. Pharm. 343, 262–269.
Xu, L., Massague, J., 2004. Nucleocytoplasmic shuttling of signal transducers. Nat. Rev. Mol. Cell. Biol. 5, 209–219.
Yang, Z., Sahay, G., Sriadibhatla, S., Kabanov, A.V., 2008. Amphiphilic block copolymers enhance cellular uptake and nuclear entry of polyplex-delivered DNA. Bioconjugate Chem. 19, 1987–1994.
Zabner, J., Fasbender, A.J., Moninger, T., 1995. Cellular and molecular barriers to gene transfer by a cationic lipid. J. Biol. Chem. 270, 18997–19007.